Column Number Density Expressions Through $M = 0$ and $M = 1$ Point Source Plumes Along Any Straight Path

Michael Woronowicz

Stinger Ghaffarian Technologies, Inc., 7701 Greenbelt Rd., Greenbelt, Maryland 20770 U.S.A.

michael.woronowicz@nasa.gov

Abstract. Analytical expressions for column number density (CND) are developed for optical line of sight paths through a variety of steady free molecule point source models including directionally-constrained effusion (Mach number $M = 0$) and flow from a sonic orifice ($M = 1$). Sonic orifice solutions are approximate, developed using a fair simulacrum fitted to the free molecule solution. Expressions are also developed for a spherically-symmetric thermal expansion ($M = 0$). CND solutions are found for the most general paths relative to these sources and briefly explored. It is determined that the maximum CND from a distant location through directed effusion and sonic orifice cases occurs along the path parallel to the source plane that intersects the plume axis. For the effusive case this value is exactly twice the CND found along the ray originating from that point of intersection and extending to infinity along the plume's axis. For sonic plumes this ratio is reduced to about 4/3. For high Mach number cases the maximum CND will be found along the axial centerline path.

Keywords: column number density, plume flows, outgassing, free molecule flow
PACS: 51.10 +y

INTRODUCTION

Providers of payloads carried aboard the International Space Station (ISS) must conduct analyses to demonstrate that any planned gaseous venting events generate no more than a certain level of material that may interfere with optical measurements from other experiments or payloads located nearby [1]. This requirement is expressed in terms of a critical maximum column number density ($\mathrm{CND}_{\mathrm{crit}}$ or σ_{crit}), with units of molecules/m^2. Depending on the level of rarefaction, such venting may be characterized by low rate effusion [2], or by a sonic distribution at higher levels. Since the relative locations of other sensitive payloads are often unknown because they may refer to future additions, this requirement becomes a search for the maximum CND along any path.

In another application, certain astronomical observations make use of CND to estimate light attenuation from a distant star through gaseous plumes, such as the "Fermi Bubbles" emanating from the vicinity of the black hole at the center of our Milky Way galaxy [3]. This allows astronomers to infer the amount of material being expelled via those plumes.

This paper presents analytical CND expressions developed for general straight paths based upon a free molecule point source model for steady effusive flow and for a distribution fitted to model flows from a sonic orifice. In this Mach number range, it is demonstrated that the maximum CND from a distant location occurs along paths parallel to the source plane that intersect the plume axis. For effusive flows this value is exactly twice the CND found along the ray originating from that point of intersection and extending to infinity along the plume's central axis. For sonic plumes this ratio is reduced to about 4/3. CND expressions are also developed for certain high M cases and more generally for a spherically-symmetric spherical expansion.

VENTING SOURCE MODEL

To describe thermally effusive and sonic orifice venting, this study uses a solution of the collisionless Boltzmann equation for fluxes from a directionally-constrained point source meant to describe directed flow from a nozzle exit over 2π steradians centered on the source normal [4]. For a source with a flow rate of $\dot{N}$ molecules/s at temperature T having cylindrical symmetry and a bulk exit velocity $\boldsymbol{u_e}$ aligned with the source normal, one finds the expression for steady state number density n at location (r, θ) simplifies to

$$n(r,\theta) = \frac{\beta \dot{N} \cos\theta}{A_1 \pi r^2} e^{w^2 - s^2} \left\{ w e^{-w^2} + \left(\frac{1}{2} + w^2 \right) \sqrt{\pi} \left(1 + \text{erf } w \right) \right\}. \tag{1}$$

In Eq. (1) $\beta \equiv 1/\sqrt{2RT}$, speed ratio $s \equiv \beta u_e$, and $w \equiv s\cos\theta$. The speed ratio is sometimes described as a molecular Mach number, where $s = \sqrt{\gamma/2}M$ and γ is the specific heat ratio for the species under consideration. Normalization factor A_1 is described by

$$A_1 \equiv e^{-s^2} + \sqrt{\pi}\, s \left(1 + \text{erf } s \right). \tag{2}$$

The column number density (CND, σ) is given by the integrated effect of the vent plume density along a given path l in free space:

$$\sigma = \int_0^\infty n \, dl \, . \tag{3}$$

With a requirement for the CND not to exceed σ_{crit}, one may use solutions of Eq. (3) to determine the physical envelope near the source where σ_{crit} is violated. One technical drawback is that Eq. (1) reaches a singularity at the source origin, so some finite critical envelope will always be predicted. However, this limitation is not consequential for systems of any practical size when such envelopes become insignificant in comparison.

EFFUSIVE (M = 0) CND EXPRESSIONS

For the case where venting occurs at such a low rate that it is characterized by a sufficiently high Knudsen number Kn with respect to the vent's diameter and there is no bulk motion (thermal effusion only), then the density field generated by Eq. (1) reduces to

$$n(r,\theta) = \frac{\dot{N} \cos\theta}{r^2 \sqrt{8\pi RT}} \, . \tag{4}$$

This case also describes the density field due to outgassing or low rate evaporation of volatile substances from a single-sided planar surface of finite dimensions when viewed from a distance, regardless of geometric details such as if the surface is a disk or a rectangle [5]. Substituting Eq. (4) into Eq. (3):

$$\sigma = \frac{\dot{N}}{\sqrt{8\pi RT}} \int_0^\infty \frac{\cos\theta}{r^2} dl \, . \tag{5}$$

1-D Centerline Path, Low Rate Effusion

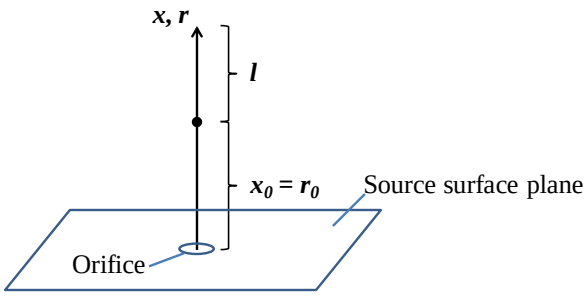

FIGURE 1. Geometry for computing CND along centerline path (1-D).

For a path that is coincident with plume axis ***x*** and begins some distance $r_0 = x_0$ from the origin, so $l = r - x_0$ and $\theta = 0$ (Fig. 1). The solution to Eq. (5) in this case is simply

$$\sigma_{cl,e}(x_0) = \frac{\dot{N}}{x_0\sqrt{8\pi RT}}. \tag{6}$$

Where the subscript "*cl,e*" represents "centerline, effusive case."

Since the density distribution is maximized along the plume axis, it is tempting to conclude Eq. (6) produces the highest level CND. However, as the results below indicate, this is not so.

2-D Path Intersecting Centerline and Source Surface Plane, Low Rate Effusion

A much more useful case involves a path that begins below the source plane, makes angle η with it as it enters the plume region at distance r_0, and intersects the plume centerline at x_0. This two dimensional case is depicted in Fig. 2 below.

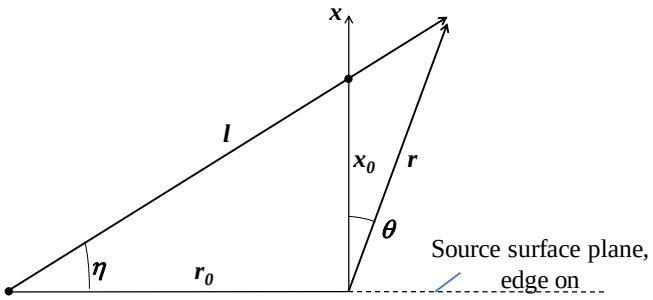

FIGURE 2. Two-dimensional CND geometry intersecting source normal and source surface plane.

Notice that $l\sin\eta = r\cos\theta$. Also, one may use the Law of Cosines to relate *r* and *l* to η. Eq. (5) becomes

$$\sigma = \frac{\dot{N}\sin\eta}{\sqrt{8\pi RT}}\int_0^\infty \frac{l\,dl}{\sqrt{\left(l^2 + r_0^2 - 2r_0 l\cos\eta\right)^3}}. \tag{7}$$

The solution to Eq. (7) is

$$\sigma = \frac{\dot{N}}{\sqrt{8\pi RT}} \frac{\sin\eta}{r_0(1-\cos\eta)} = \sigma_{cl,e} \frac{\tan\eta \sin\eta}{1-\cos\eta} . \tag{8}$$

Taking the derivative of Eq. (8) with respect to inclination angle η, one finds the highest values for σ occur when $\eta = 0$. Under these circumstances, one may imagine r_0 stretches out to infinity. In this limit it is a vanishingly small distortion of the right triangle comprised of η, x_0, and r_0 to imagine it describing a path that is actually parallel to the source plane at a height of x_0 instead of intersecting it at some exceedingly distant point r_0. Applying L'Hospital's Rule to Eq. (8) for $\eta = 0$ yields

$$\sigma(\eta \to 0) \to 2\sigma_{cl,e} . \tag{9}$$

This special limiting case may be confirmed by evaluating Eq. (5) directly across a horizontal path x_0 above the source surface, extending to infinity in both directions. Due to symmetry, an observer at x_0 for this type of source would measure the same CND along and perpendicular to the plume axis.

3-D General Path, Low Rate Effusion

When the CND column density integration path does not intersect the source normal axis, evaluation of Eq. (5) becomes more complex. Using Fig. 3 below, one finds that the plane containing ***r*** and ***l*** defines the triangle for application of the Law of Cosines involving angle η, but as this plane is inclined at angle θ off the plume axis one cannot use quantities contained within that plane to provide a useful relationship containing θ. By taking the dot product of ***l*** with ***x*** to define path inclination angle ω, another plane parallel to the plume axis may be constructed, and

$$\boldsymbol{r}\cos\theta = \boldsymbol{l}\sin\omega + \boldsymbol{r_0}\cos\theta_0 . \tag{10}$$

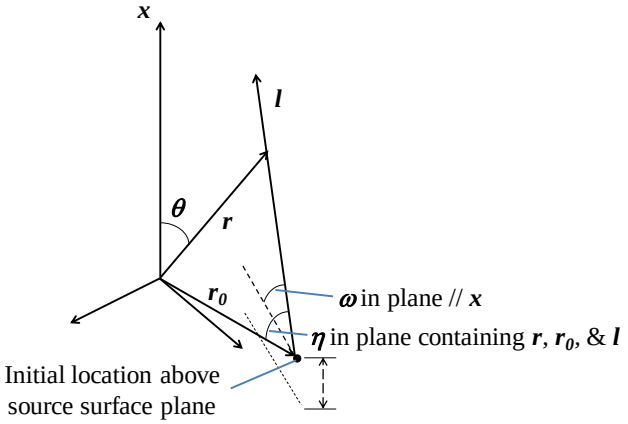

FIGURE 3. 3-D CND path originating above source surface plane.

The vertical components of ***r*** measured from the source origin is recast in terms of parameters viewed from the beginning of the path origin. Since $\boldsymbol{r_0}$ emanates from the source origin, its length contribution viewed from ***l*** is negative. The integral for this case is similar to Eq. (7), yielding

$$\sigma = \frac{\dot{N}}{\sqrt{8\pi RT}} \frac{\sin\omega - \cos\theta_0}{r_0(1-\cos\eta)} . \tag{11}$$

When the path begins in the source plane or below it, $\theta_0 = \pi/2$. Eq. (11) is maximized when the path intersects the source surface plane and ω and η both equal zero, and the configuration simplifies to that from the previous section.

SONIC ORIFICE (M = 1) CND EXPRESSIONS

Unfortunately the form of Eq. (1) is too complicated to integrate analytically when M = 1, so it was replaced by a fit curve having a simpler analytical form. Based on evaluation of Eq. (1) for monatomic, diatomic, and certain polyatomic molecules, it was found the angular distribution was generally enveloped between $\cos^3\theta$ and $\cos^4\theta$ (Fig. 4).

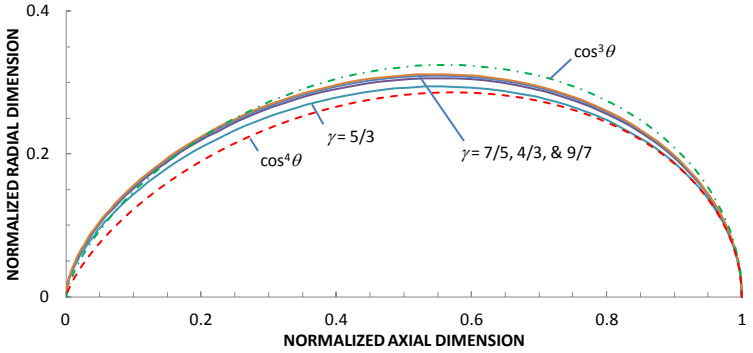

FIGURE 4. Plume model contours at M = 1 for gases having various specific heat ratios.

Based on consideration of the ISS maximum CND requirement, it was decided to match the centerline value of Eq. (1) and to replace the angular distribution by $\cos^3\theta$. Without much distortion, approximate sonic orifice solutions in this study (subscript "s") will be described by

$$n_s(r,\theta) \approx K\frac{\cos^3\theta}{r^2}, \quad \text{where} \quad K \equiv \frac{\beta\dot{N}}{\pi}\left\{\frac{\sqrt{\frac{\gamma}{2}}\,e^{-\frac{\gamma}{2}} + \left(\frac{\gamma+1}{2}\right)\sqrt{\pi}\left(1+\text{erf}\sqrt{\frac{\gamma}{2}}\right)}{e^{-\frac{\gamma}{2}} + \sqrt{\frac{\pi\gamma}{2}}\left(1+\text{erf}\sqrt{\frac{\gamma}{2}}\right)}\right\}. \tag{12}$$

1-D Centerline Path, Sonic Orifice Case

Figure 1 provides the geometric description for this configuration, and substitution of Eq. (12) into Eq. (3) yields

$$\sigma_{cl,s} = \frac{K}{x_0}. \tag{13}$$

The similarity between Eq. (13) and Eq. (6) is clear if one were to replace the product of all factors outside the integral of Eq. (5) by K.

2-D Path Intersecting Centerline and Source Surface Plane, Sonic Orifice Case

If one were to apply the geometric relationship $l\sin\eta = r\cos\theta$ in Fig. 2 to Eq. (12), the resulting CND becomes

$$\sigma_s = \frac{K}{3r_0 \sin\eta}\left[2(1+\cos\eta)+\frac{1}{2}\sin\eta\sin 2\eta\right] = \frac{\sigma_{cl,s}}{3\cos\eta}\left[2(1+\cos\eta)+\frac{1}{2}\sin\eta\sin 2\eta\right]. \tag{14}$$

As $\eta \to 0$ for the same geometric considerations discussed regarding the effusive case:

$$\sigma(\eta \to 0) \to \frac{4}{3}\sigma_{cl,s}. \tag{15}$$

This result may be found directly by computing the integral for the corresponding transverse optical path that intersects the plume axis at x_0. Since this result is true for an enveloping curve fit to Eq. (1) under sonic conditions, Eq. (15) should be considered an approximate relationship.

Maximum CND Observations for Higher Mach Number Sources

Incidentally, reviewing the approach taken to fit an axisymmetric plume's angular distribution to some power *m* of the cosine function,

$$n(r,\theta) \approx \tilde{K}\frac{\cos^m\theta}{r^2}, \tag{16}$$

it is noted that the axial case, beginning at $r = x_0$ and independent of θ, yields $\sigma_{cl} = \tilde{K}/x_0$. From previous results, one might be tempted to assume the distant-limit transverse CND follows a progression of $\sigma/\sigma_{cl} = (m+1)/m$, however straightforward application of Eq. (3) for this path results in [6]

$$\sigma = \tilde{K}\int_{-\infty}^{\infty}\frac{\cos^m\theta}{r^2}dl = \sigma_{cl}\left[2\int_0^{\infty}\frac{ds}{\left(1+s^2\right)^{\frac{m+2}{2}}}\right] = \sigma_{cl}B\left(\frac{1}{2},\frac{m+1}{2}\right) = \sqrt{\pi}\sigma_{cl}\frac{\Gamma\left(\frac{m+1}{2}\right)}{\Gamma\left(\frac{m+2}{2}\right)}. \tag{17}$$

For integer values of *m* < 6 the results of Eq. (17) exceed unity, meaning a transverse path from a distant location intersecting the plume axis will experience a higher CND than an axial path from that intersection point outwards. For higher integer values of *m* this observation no longer holds. The axial CND then provides the maximum value for evaluating ISS requirements.

3-D General Path, Sonic Orifice Case

Continuing with the setup depicted in Fig. 3 and applying Eq. (10) to relate *r* and θ to *l*, eventually one obtains

$$\sigma = \frac{\sigma_{cl,s}\tan\eta}{3(1-\cos\eta)^2}\left\{\frac{\sin^3\omega\left(2+3\cos\eta-\cos^3\eta\right)}{(1+\cos\eta)^2} - 3\sin^2\omega\cos\theta_0 + 3\sin\omega\cos^2\theta_0 - \cos^3\theta_0(2-\cos\eta)\right\}. \tag{18}$$

In the limit where $\theta_0 \to \pi/2$, $\omega = \eta$, and $\eta \to 0$, we recover Eq. (15).

RADIAL POINT SOURCE SOLUTIONS

To describe gas being liberated from a source with no directional constraints and no bulk velocity, this study uses a solution of the collisionless Boltzmann equation developed by Narasimha [7]. Under these conditions (subscript "*r*")

$$n_r(r) = \frac{\dot{N}}{\pi r^2 \sqrt{8\pi RT}}. \tag{19}$$

A general CND path geometry is depicted in Fig. 5 below. In this arrangement there is no source surface plane or plume axis, but there is a length r_0 separating the initial location from the spherically-symmetric source.

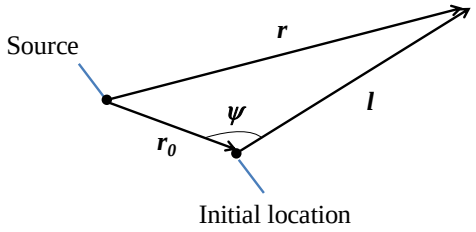

FIGURE 5. Geometry for evaluating CND due to a radial point source.

For angle ψ between $\boldsymbol{r_0}$ and $\boldsymbol{l}$ the Law of Cosines may be applied to produce

$$\sigma = \frac{\dot{N}}{\pi r_0 \sqrt{8\pi RT}} \frac{\pi - \psi}{\sin\psi}. \tag{20}$$

The product $r_0 \sin\psi$ represents the minimum distance between the path and the source for Fig. 5 geometry x_0. When $\psi = \pi$ Eq. (20) produces the radial solution for a path traveling away from the source

$$\sigma(\psi = \pi) = \sigma_r = \frac{\dot{N}}{\pi r_0 \sqrt{8\pi RT}}, \tag{21}$$

and when $\psi = \pi/2$ the path begins in a direction at right angles to the local flowfield and

$$\sigma\left(\psi = \frac{\pi}{2}\right) = \frac{\pi}{2}\sigma_r. \tag{22}$$

The maximum CND for a path that extends to infinity in both directions and approaches the origin no closer than r_0 is twice the value of Eq. (22).

CONCLUDING REMARKS

A study was undertaken to determine closed form analytical solutions for a number of CND configurations frequently encountered and otherwise performed numerically using intuition. It was observed for CNDs associated with paths in the presence of low-rate effusive venting and higher-rate sonically-constrained discharges that maximum CNDs should occur along paths parallel to the source plane that intersect the plume axis. Furthermore,

maximum CNDs for paths immersed in presence of an unconstrained radial source do not lie along radial trajectories.

Working with fit curves in the form of $\cos^m \theta$, it was further determined for integer values of $m > 5$, approximating the behavior of spacecraft thruster plumes, that maximum CND values switched from transverse to axial paths.

It is hoped that use of these solutions will greatly reduce the amount of effort needed to assess CNDs for a variety of applications ranging from satisfying spacecraft requirements to making astronomical assessments.

ACKNOWLEDGMENTS

The author gratefully acknowledges support from NASA Contract NNG12CR31C, especially Mr. Benjamin Reed, NASA-GSFC Code 408, Ms Kristina Montt de Garcia and Mr. David Hughes, NASA-GSFC Code 546, and Dr. Dong-Shiun Lin and Ms Cori Quirk, SGT, Inc.

REFERENCES

1. *Attached Payload Interface Requirements Document, International Space Station Program, SSP 57003*, Rev. H, p. 3-61, October 2011.
2. S-H Li, J. Fan, and Y-H Shu, "A Breakdown Criterion of Free Molecular Flows and an Optimum Analysis of EBPVD," in *26th International Symposium on Rarefied Gas Dynamics*, AIP Conference Proceedings 1084, edited by T. Abe (American Institute of Physics, Melville, NY, 2009), pp. 1105–1110.
3. A. J. Fox, *et al.*, "Probing the Fermi Bubbles in Ultraviolet Absorption...," Astrophysical Journal Letters, **799**, L7 (2015).
4. M. Woronowicz, "Highlights of Transient Plume Impingement Model Validation and Applications," *AIAA Paper No. 2011-3772*, 42nd AIAA Thermophysics Conference, Honolulu, HI, 27-30 June 2011.
5. C. Cai, "High speed plume farfield density properties," in *29th International Symposium on Rarefied Gas Dynamics*, AIP Conference Proceedings 1628, edited by J. Fan (American Institute of Physics, Melville, NY, 2014), pp. 563–568.
6. I.S. Gradshteyn, I. M. Ryzhik, *Table of Integrals, Series, and Products* (Academic Press, San Francisco, 1980), p. 948.
7. R. Narasimha, "Collisionless Expansion of Gases Into Vacuum," J. Fluid Mech., **12**, pp. 294-308 (1962).